Franck–Condon simulation of the single vibronic level emission spectra of HSiF and DSiF including anharmonicity

Daniel K. W. Mok,[a] Edmond P. F. Lee, and Foo-tim Chau
Department of Applied Biology and Chemical Technology, Hong Kong Polytechnic University, Hung Hom, Hong Kong

John M. Dyke
Department of Chemistry, University of Southampton, Highfield, Southampton SO17 1BJ, United Kingdom

Potential energy functions (PEFs) of the $\tilde{X}\,^1A'$ and $\tilde{A}\,^1A''$ states of HSiF have been computed using the coupled-cluster single-double plus perturbative triple excitations and complete-active-space self-consistent-field multireference internally contracted configuration interaction methods, respectively, employing augmented correlation-consistent polarized-valence quadruple-zeta basis sets. For both electronic states of HSiF and DSiF, anharmonic vibrational wavefunctions and energies of all three modes have been calculated variationally with the *ab initio* PEFs and using Watson's Hamiltonian for nonlinear molecules. Franck–Condon factors between the two electronic states, allowing for Duschinsky rotation, were computed using the calculated anharmonic vibrational wavefunctions. These Franck–Condon factors were used to simulate the single vibronic level (SVL) emission spectra recently reported by Hostutler *et al.* in J. Chem. Phys. **114**, 10728 (2001). Excellent agreement between the simulated and observed spectra was obtained for the $\tilde{A}\,^1A''(1,0,0)\rightarrow\tilde{X}\,^1A'$ SVL emission of HSiF. Discrepancies between the simulated and observed spectra of the $\tilde{A}\,^1A''(0,1,0)$ and $(1,1,0)$ SVL emissions of HSiF have been found. These are most likely, partly due to experimental deficiencies and, partly to inadequacies in the *ab initio* levels of theory employed in the calculation of the PEFs. Based on the computed Franck–Condon factors, minor revisions of previous vibrational assignments are suggested. The calculated anharmonic wave functions of higher vibrational levels of the $\tilde{X}\,^1A'$ state show strong mixings between the three vibrational modes of HSi stretching, bending, and SiF stretching. © *2004 American Institute of Physics.* [DOI: 10.1063/1.1630559]

I. INTRODUCTION

Recently, Hostutler *et al.* (HCJ01)[1] reported single vibronic level (SVL) $\tilde{A}\,^1A''\rightarrow\tilde{X}\,^1A'$ emission spectra of jet-cooled HSiF and DSiF. In this spectroscopic study, these authors attempted to confirm the assignment of the observed spectra by spectral simulation, employing Franck–Condon (FC) profiles computed within the harmonic oscillator approximation. However, it was found that, apart from the $\tilde{A}\,^1A''(0,0,0)\rightarrow\tilde{X}\,^1A'$ SVL emission band, the simulated emission spectra of HSiF did not agree very well with the observed spectra. The discrepancies between simulated and observed spectra were attributed to the significant coupling between the HSi stretching (ν_1) and bending (ν_2) modes, which was not accounted for in the harmonic oscillator model employed in the calculation of the FC factors. At the end of the discussion in HCJ01,[1] a call was made for spectral simulations, which would include the effects of anharmonicity, and it was proposed that the reported HSiF and DSiF spectra would provide rather stringent tests of such calculations. The present theoretical investigation is a direct response to this request and challenge.

Prior to the dispersed fluorescence study of HCJ01 on HSiF and DSiF, Clouthier and co-workers have published two extensive rotationally resolved laser induced fluorescence (LIF) studies[2,3] on HSiF and/or DSiF. From these three spectroscopic studies of the Clouthier group,[1–3] equilibrium geometrical parameters, harmonic and fundamental vibrational frequencies of the $\tilde{X}\,^1A'$ and $\tilde{A}\,^1A''$ states of HSiF (and DSiF) have been derived or measured. Earlier spectroscopic and *ab initio* studies on HSiF and/or DSiF, and the importance of the silylene family of reactive intermediates in chemical vapor deposition processes in the semiconductor industry have been discussed previously (see Refs. 1, 2, and 3 and references therein) and hence will not be repeated here. After HCJ01 had appeared, Christiansen *et al.*[4] reported coupled-cluster calculations on the $\tilde{X}\,^1A'$ and $\tilde{A}\,^1A''$ states of HSiF, FC factor calculations within the multidimensional harmonic oscillator model, and simulated $\tilde{A}\,^1A''\leftarrow\tilde{X}\,^1A'$ absorption spectra obtained at different levels of coupled-cluster response theory. The highest levels of *ab initio* calculation carried out in Ref. 4 on HSiF are the CCSD/aug-cc-pVTZ level for geometry, harmonic vibrational frequencies, and spectral simulation, and the CC3/aug-cc-pVQZ level for vertical excitation energy. These *ab initio* calculations on the two electronic states of HSiF were of the highest levels avail-

---
[a]Author to whom correspondence should be addressed; electronic mail: bcdaniel@polyu.edu.hk

J. Chem. Phys., Vol. 120, No. 3, 15 January 2004

Simulated spectra of HSiF 1293

able prior to the present study. The simulated $\tilde{A}\,^1A''$ $\leftarrow \tilde{X}\,^1A'$ spectra were compared with the LIF spectrum of Ref. 3 and it was noted in Ref. 4 that "there are aspects of the weaker features where the calculated intensity pattern does not match the experimental results." Again, the inadequacy of the harmonic oscillator approximation was identified as one of the probable causes of the discrepancies between theory and experiment, particularly for the higher energy region of the spectrum. No attempt, however, has been made in Ref. 4 to simulate the SVL emission spectra of HSiF and DSiF reported in HCJ01.

We have shown recently that the inclusion of anharmonicity in the theoretical method of FC simulation has significant effects on the simulated SVL emission spectra of CF_2,[5] and some bands in the photoelectron spectra of F_2O and Cl_2O.[6,7] Theoretically, the inclusion of anharmonicity should improve the reliability of the simulated spectra, and generally, simulated spectra including anharmonicity match better with observed spectra than those obtained within the harmonic oscillator model, as expected. In the case of HSiF, in addition to possible coupling among the three vibrational modes mentioned above, anharmonicity is expected to be particularly large for the HSi stretching mode. The present investigation on the SVL emission spectra of HSiF and DSiF is our first attempt to employ the anharmonic FC method to study a species of C_S symmetry, where all three vibrational modes belonging to the same irreducible representation are included in the FC factor calculation, and also to study a triatomic species containing a hydrogen atom, which is expected to show strongly anharmonicity in the stretching mode involving the hydrogen atom.

II. THEORETICAL METHODS AND COMPUTATIONAL DETAILS

Ab initio energy scans on the $\tilde{X}\,^1A'$ and $\tilde{A}\,^1A''$ states of HSiF were carried out for the fitting of their potential energy functions (PEFs). The coupled-cluster single and double[8] plus perturbative triple[9] excitations [CCSD(T)] method, which is known to be one of the best single-reference correlation methods, was employed for calculations on the closed-shell $\tilde{X}\,^1A'$ state. For the $\tilde{A}\,^1A''$ state, which is an open-shell singlet state (see Ref. 2) and cannot be described adequately by a single configuration wavefunction, complete-active-space self-consistent-field[10] multireference internally contracted configuration interaction[11] (CASSCF/MRCI) calculations were carried out. The aug-cc-pVQZ basis set[12] was employed and the core electrons were frozen in both the CCSD(T) and CASSCF/MRCI calculations. In the CASSCF and MRCI calculations of the $\tilde{A}\,^1A''$ state, the full valence molecular orbital space was active, giving ~112.9 million uncontracted configurations and ~1.3 million internally contracted configurations in the MRCI calculations. 388 CCSD(T) energy points in the ranges of $1.1 \leq r(\text{HSi})$ ≤ 2.3 Å, $40.0 \leq \theta(\text{HSiF}) \leq 155.0°$, and $1.4 \leq r(\text{SiF})$ ≤ 1.95 Å were scanned for the $\tilde{X}\,^1A'$ state, and 206 CASSCF/MRCI energy points in the ranges of $1.1 \leq r(\text{HSi})$ ≤ 2.35 Å, $40.0 \leq \theta(\text{HSiF}) \leq 170.0°$, and $1.45 \leq r(\text{SiF})$

≤ 1.8 Å were scanned for the $\tilde{A}\,^1A''$ state. All the *ab initio* calculations were carried out using the MOLPRO suite of programs.[13] The following polynomial was fitted to the calculated *ab initio* total energies mentioned above to give the PEFs of the $\tilde{X}\,^1A'$ and $\tilde{A}\,^1A''$ states of HSiF:

$$V = \sum_{ijk} C_{ijk}(S_1)^i(S_2)^j(S_3)^k + V_{eqm}. \quad (1)$$

The bending coordinate suggested by Carter and Handy[14]

$$S_2 = \Delta\theta + \alpha\Delta\theta^2 + \beta\Delta\theta^3$$

has been employed for S_2, where $\Delta\theta$ is the displacement of the bond angle from the equilibrium value, $(\theta - \theta_e)$, while S_1 and S_3 are the displacements of the HSi and SiF bond lengths from the equilibrium values $(r - r_e)$, respectively.

The fitting of the PEFs, the variational calculations of the anharmonic vibrational wavefunctions and the FC factor calculations were performed as described previously[5–7] and hence the full description of the methods will not be repeated here. In brief, Watson's Hamiltonian[15,16] for a nonlinear molecule was used, and both anharmonicity and Duschinsky rotation were included in the FC factor calculations. Here, only some technical details specific to the present study are given; these are as follows. Anharmonic vibrational wave functions were expressed as linear combinations of harmonic oscillator functions, $h(\nu_1,\nu_2,\nu_3)$, where ν_1, ν_2, and ν_3 denote the quantum numbers of the harmonic basis functions for the HSi stretching, bending, and SiF stretching modes, respectively. Harmonic basis functions with vibrational quantum numbers of up to $h(10,15,12)$ and a restriction of $\nu_1 + \nu_2 + \nu_3 < 15$, were included in the variational calculations of the $\tilde{X}\,^1A'$ state, giving a total of 771 anharmonic vibrational states. For the $\tilde{A}\,^1A''$ state, harmonic basis functions of up to $h(12,12,8)$, with a restriction of $\nu_1 + \nu_2 + \nu_3 < 12$ and a total of 435 anharmonic vibrational states were considered.

The iterative Franck–Condon analysis (IFCA) procedure was carried out (see Refs. 5 and 6 for details), with the geometry of the $\tilde{X}\,^1A'$ state fixed to the most recent estimated equilibrium (r_e^z) geometry of HCJ01,[1] while the geometrical parameters of the $\tilde{A}\,^1A''$ state were varied systematically, until the best match between simulated and observed SVL emission spectra was obtained (see also Sec. III for a more detailed description, which includes the *ab initio* calculations). Vibronic components in the SVL $\tilde{A}\,^1A'' \rightarrow \tilde{X}\,^1A'$ emission spectra of HSiF/DSiF were simulated using Gaussian functions with a full width at half-maximum (FWHM) of 30 cm^{-1}, which is a spectral resolution slightly better than that of the observed SVL emission spectra of HCJ01.[1] The relative intensity of each vibrational component in a simulated spectrum is given by the corresponding computed anharmonic FC factor and a frequency factor of power 4.

III. RESULTS AND DISCUSSION

The computed results are summarized in Tables I–V and the simulated spectra are shown in Figs. 1–6. They are discussed in the following subsections.

TABLE I. The CCSD(T)/aug-cc-pVQZ and CASSCF/MRCI/aug-cc-pVQZ PEFs of the $\tilde{X}\,^1A'$ and $\tilde{A}\,^1A''$ states of HSiF [see text and Eq. (1)].

$C(i,j,k)$	$\tilde{X}\,^1A'$	$\tilde{A}\,^1A''$
002	0.5754	0.5905
200	0.2644	0.2195
020	0.1098	0.0511
101	0.0284	−0.0130
011	0.0526	0.0277
110	−0.0016	0.0184
003	−1.2010	−1.1254
300	−0.4064	−0.4553
030	0.0051	−0.0053
102	−0.0503	0.0105
012	−0.0588	0.0128
201	0.0018	−0.0076
210	−0.0041	−0.0080
021	−0.0958	−0.0498
120	−0.0497	−0.0788
111	−0.0795	−0.0247
004	1.2358	0.8308
400	0.4348	0.4599
040	0.0429	0.0816
103	0.0459	−0.0834
013	0.0033	−0.4703
301	−0.0078	0.0213
310	−0.0020	0.0378
031	0.0426	0.0753
130	−0.0054	−0.0053
202	0.0186	0.1551
022	0.0090	−0.0024
220	−0.0357	−0.0310
112	0.1210	0.0315
211	0.0187	0.1905
121	0.1067	0.1560
500	−0.3562	−0.3528
600	0.1459	0.1576
050	0.0278	0.1705
060	−0.0035	−0.3258
140	−0.0196	0.0725
230	0.0050	0.1289
320	0.0350	0.1934
410	−0.0019	−0.0376
150	−0.0149	0.0675
240	−0.0175	0.1100
330	0.0208	−0.1722
420	−0.0133	−0.3216
510	0.0078	−0.0832
070	−0.0305	−0.6236
080	0.0381	0.4384
090	0.0997	1.1403
0,10,0	0.0420	0.4883
α	−0.0495	−0.1821
r(H–Si)	1.5291	1.5227
∠(HSiF)	96.7093	116.7147
r(Si–F)	1.6127	1.6194

A. Potential energy functions and anharmonic vibrational wave functions

The CCSD(T) and CASSCF/MRCI PEFs of the $\tilde{X}\,^1A'$ and $\tilde{A}\,^1A''$ states of HSiF, respectively, are given in Table I. The root mean square (rms) deviation of the fitted potential from the computed single point energies is below 10 cm^{-1} for the CCSD(T)/aug-cc-pVQZ PEF of the $\tilde{X}\,^1A'$ state. For the CASSCF/MRCI/aug-cc-pVQZ PEF of the $\tilde{A}\,^1A''$ state,

the rms deviation is 20 cm^{-1}. Table II shows the computed anharmonic vibrational energies and wave functions of some low-lying vibrational levels of the $\tilde{X}\,^1A'$ and $\tilde{A}\,^1A''$ electronic states and also some higher energy vibrational levels of the $\tilde{X}\,^1A'$ state. For both electronic states of HSiF considered, the anharmonic vibrational wave functions, expressed as linear combinations of the harmonic basis functions, show that anharmonicity is not negligible even for the low-lying vibrational levels and the three harmonic modes of HSi stretch, bending and SiF stretch show significant coupling.

The calculated anharmonic vibrational energies and wave functions of some higher energy levels of the $\tilde{X}\,^1A'$ state are shown in Table II as examples. It can be seen that these anharmonic vibrational levels, which have their leading harmonic basis functions of $h(1,\nu_2'',\nu_3'')$ with the same $(\nu_2'' + \nu_3'')$ values, are calculated to be very close in energies. The computed energy differences of these levels are less than 30 cm^{-1} in most cases. This is because the differences between the observed (computed) fundamental frequencies of the bending and SiF stretching modes of the $\tilde{X}\,^1A'$ state of HSiF are only 21.3 (15) cm^{-1}, respectively (see Table IV and later text). These energy differences of less than 30 cm^{-1} are smaller than the FWHM used in the simulated spectra mentioned above. Consequently, vibrational components arising from SVL emissions to these vibrational levels, which are calculated to be closer in energy than 30 cm^{-1}, would not be resolved in the simulated spectra, but appear as a single, overlapped band. Similarly, since the resolution of the observed spectra are slightly poorer than that used in the simulated spectra (see Figs. 1, 3, 4, 5, and 6), vibrational components with calculated energy separations of less than 30 cm^{-1} would not be expected to be resolved in the observed spectra. Detailed discussions on the vibrational assignments of overlapping vibrational series in the observed SVL emission spectra of HSiF will be given in the subsection dealing with spectral simulation. This problem of overlapping vibrational components of the bending and SiF stretching series, however, is not present in the SVL emission spectra of DSiF, because the bending and SiF stretching fundamental frequencies of the $\tilde{X}\,^1A'$ state of DSiF, observed or calculated, differ by over 200 cm^{-1} (see Table IV).

From the calculated anharmonic vibrational wave functions of the higher energy levels of the $\tilde{X}\,^1A'$ state of HSiF shown in Table II, it can be seen that there are very strong mixings among harmonic basis functions of all three vibrational modes of HSi stretching, bending and SiF stretching, particularly for the combination band manifolds, which have the same ν_1'' and $\nu_m'' = \nu_2'' + \nu_3''$, and they are very close in energy, as discussed above. Consequently, based solely on the computed leading harmonic basis functions of the anharmonic wave functions, the vibrational designations of these anharmonic vibrational levels are not unambiguously clear, because of strong mixings of the harmonic basis functions in the anharmonic vibrational wave functions. In order to assist the labeling of the vibrational quantum numbers, some two-dimensional cross-section plots of the computed anharmonic vibrational wave functions of these vibrational levels between pairs of normal mode coordinates have been exam-

TABLE II. The computed anharmonic vibrational energies (E_{vib} in cm^{-1} relative to the ground vibrational state) and wave functions (in terms of the harmonic basis functions; see text) of some low-lying vibrational levels of the $\tilde{X}\,^1A'$ and $\tilde{A}\,^1A''$ electronic states of HSiF, and some higher energy levels of the $\tilde{X}\,^1A'$ state (see text).

E_{vib}	Anharmonic vibrational wave function
$\tilde{X}\,^1A'$	(Some higher levels)
4461.158	$-0.6193h(1,2,1)-0.3698h(1,3,0)-0.3387h(1,1,2)$ $+0.2763h(0,4,1)+0.2565h(0,5,0)$
4444.442	$0.5982h(1,1,2)-0.4239h(1,3,0)+0.3184h(0,5,0)$ $-0.2687h(2,1,0)+0.2358h(1,0,3)$
4432.019	$-0.4661h(1,2,1)+0.3671h(1,3,0)+0.3421h(1,0,3)+$ $-0.2852h(0,5,0)+0.2661h(1,1,2)$
4423.953	$0.6735h(1,0,3)-0.3745h(1,1,2)+0.3246h(1,0,4)$ $-0.2371h(1,0,2)+0.1924h(1,2,1)$
3626.938	$0.6628h(1,1,1)+0.4991h(1,2,0)+0.2660h(1,0,2)$ $-0.2474h(0,4,0)-0.1964h(0,3,1)$
3610.083	$-0.6072h(1,0,2)+0.5468h(1,2,0)-0.2864h(0,4,0)$ $-0.2141h(1,1,1)-0.1968h(1,0,3)$
3598.737	$0.5699h(1,0,2)-0.5485h(1,1,1)+0.3525h(1,2,0)$ $+0.2001h(0,3,1)-0.1893h(0,4,0)$
	(Low-lying levels)
1930.830	$-0.9345h(1,0,0)+0.2634h(2,0,0)+0.1841h(0,2,0)$ $-0.0913h(0,0,0)+0.0650h(4,0,0)$
1712.708	$0.9646h(0,2,0)+0.1827h(1,0,0)+0.1391h(0,2,1)$ $-0.0800h(0,3,0)+0.0444h(0,1,0)$
1699.996	$-0.9547h(0,1,1)-0.2241h(0,1,2)+0.1239h(0,0,2)$ $+0.1042h(0,1,0)+0.0577h(1,1,1)$
1677.423	$0.9122h(0,0,2)+0.3104h(0,0,3)-0.1838h(0,0,1)$ $+0.1070h(0,1,1)-0.0871h(1,0,2)$
859.647	$0.9892h(0,1,0)+0.1078h(0,1,1)-0.0589h(1,1,0)$ $-0.0412h(0,2,0)+0.0361h(0,0,1)$
845.030	$-0.9733h(0,0,1)-0.1812h(0,0,2)+0.0906h(1,0,1)$ $+0.0725h(0,0,0)+0.0395h(0,1,0)$
0.000	$0.9923h(0,0,0)-0.0906h(1,0,0)+0.0720h(0,0,1)$ $-0.0295h(3,0,0)+0.0164h(0,0,3)$
$\tilde{A}\,^1A''$	(Low-lying levels)
2128.492	$-0.8628h(1,1,0)-0.3170h(2,1,0)-0.1547h(3,1,0)$ $-0.1372h(4,1,0)-0.1138h(1,1,1)$
2009.066	$-0.9419h(0,2,1)-0.2240h(0,2,2)+0.1026h(0,2,0)$ $-0.1018h(0,3,0)+0.0820h(1,0,1)$
1719.216	$-0.9555h(0,3,0)+0.1479h(1,1,0)-0.1190h(0,3,1)$ $+0.1055h(0,4,0)-0.0757h(2,3,0)$
1702.117	$-0.9066h(0,0,2)-0.3202h(0,0,3)+0.1962h(0,0,1)$ $-0.1126h(1,0,2)-0.0742h(0,0,4)$
1606.496	$0.8708h(1,0,0)+0.3686h(2,0,0)+0.1484h(3,0,0)$ $-0.1372h(0,0,0)+0.1328h(4,0,0)$
1436.560	$-0.9610h(0,1,1)-0.2082h(0,1,2)+0.0921h(0,1,0)$ $-0.0834h(1,1,1)-0.0505h(0,2,0)$
1159.644	$-0.9800h(0,2,0)-0.1050h(0,2,1)+0.0844h(1,0,0)$ $-0.0575h(2,2,0)+0.0549h(0,3,0)$
857.667	$-0.9657h(0,0,1)-0.1916h(0,0,2)-0.1232h(1,0,1)$ $+0.0807h(0,0,0)-0.0466h(3,0,1)$
582.819	$-0.9874h(0,1,0)-0.0916h(0,1,1)-0.0910h(1,1,0)$ $-0.0484h(3,1,0)-0.0426h(2,1,0)$
0.000	$0.9858h(0,0,0)+0.1297h(1,0,0)+0.0791h(0,0,1)$ $+0.0477h(3,0,0)+0.0324h(2,0,0)$

ined. The quantum numbers of a vibrational level were determined according to the numbers of nodes the computed wave function has along the respective normal mode coordinate. These plots for low-lying vibrational levels of the $\tilde{X}\,^1A'$ state suggest that within a combination manifold of ν''_m, the levels with larger ν''_3 are lower in energy. However, for higher vibrational states, the nodal structures of the calculated anharmonic vibrational wave functions become less

clear from the plots. Nevertheless, these higher vibrational states are labeled according to the empirical observation in the low-lying vibrational levels that, within a combination manifold of ν''_m, the levels with larger ν''_3 are lower in energy. It should be noted, however, that, with such strong mixings of the harmonic basis functions in the anharmonic vibrational wave functions, as shown for the higher energy vibrational levels of the $\tilde{X}\,^1A'$ state of HSiF given in Table

TABLE III. The computed and experimentally derived geometrical parameters[a] of the $\tilde{X}\,^1A'$ and $\tilde{A}\,^1A''$ states of HSiF.

	HSi/Å	HSiF/(deg)	SiF/Å	Reference
$\tilde{X}\,^1A'$				
CCSD(T)/aug-cc-pVQZ	1.5291	96.7	1.6127	Present
CAS/TZ(2df,2pd)	1.521	97.1	1.618	GG[b]
CCSD/TZ(2df,2pd)	1.528	96.8	1.615	GG[c]
CCSD/aug-cc-pVTZ	1.531	96.5	1.620	4[d]
Effective r_0	1.548(3)	97.0(6)	1.606(1)	3
Average r_z	1.542(2)	96.9(4)	1.608(1)	3
Estimated equilibrium r_e^z	1.528(5)	96.9(5)	1.603(3)	3[e]
Average r_z	1.542(2)	96.9(3)	1.6076(5)	1
Estimated equilibrium r_e^z	1.529(6)	96.9(3)	1.603(1)	1[e]
$\tilde{A}\,^1A''$				
CASSCF/MRCI/aug-cc-pVQZ	1.5227	116.7	1.6194	Present
CAS/TZ(2df,2pd)	1.571	114.5	1.607	GG[b]
MRCI/TZ(2df,2pd)	1.535	114.9	1.617	GG[c]
CCSD/aug-cc-pVTZ	1.527	115.2	1.614	4[d,f]
Semirigid bender r_e	1.547 57(21)	[114.5][g]	1.601 50(16)	2
Effective r_0	1.557(1)	114.4(3)	1.602(1)	3
Equilibrium r_e	1.526(14)	115.0(6)	1.597(3)	3
Average r_z	1.555(4)	114.3(5)	1.603(1)	3
Estimated equilibrium r_e^z	1.536(5)	114.3(5)	1.598(3)	3[e]
IFCA	1.526[h]	116.0	1.597[h]	Present

[a]Equilibrium geometrical parameters, unless otherwise stated; estimated uncertainties/errors given in parentheses (see original works for details); for earlier works see Ref. 2 and references therein.
[b]K. J. Gregory and R. S. Grev (unpublished), quoted in Refs. 2 and 4.
[c]K. J. Gregory and R. S. Grev (unpublished), quoted in Refs. 1 and 3.
[d]The highest level of calculation in this work.
[e]Obtained from the r_z structure, see original works for details; the bond angles were assumed to be the same in the r_z and r_e^z structures.
[f]Excited state calculations by coupled cluster response theory.
[g]Fixed to the *ab initio* value.
[h]Fixed to the experimentally derived r_e values; see text.

TABLE IV. Computed and observed vibrational frequencies[a] (cm^{-1}) of the $\tilde{X}\,^1A'$ state of HSiF and DSiF.

	ω_1(SiH)	ω_2(bend)	ω_3(SiF)	ν_1	ν_2	ν_3	Reference
HSiF $\tilde{X}\,^1A'$							
CCSD(T)/aug-cc-pVQZ	2006	876	861	1931	860	845	Present
CAS/TZ(2df,2pd)	2083	929	848	⋯	⋯	⋯	GG[b]
CCSD/aug-cc-pVTZ	2015	877	847	⋯	⋯	⋯	4
IR matrix	⋯	⋯	⋯	1913.1	859.0	833.7	18
Fitted HFF (calc.)[c]	1977.3	861.0	843.1	⋯	⋯	⋯	3
Emissions ($\omega_i^{0''}$)[d]	1964.8(25)	863.72(55)	838.4(21)	1931.6	859.7	838.4	1
Observed (ω_i)[e]	2009.0(30)	876.0(10)	838.4(50)	⋯	⋯	⋯	1
Fitted HFF (calc.)[c]	2008.4	876.4	838.6	⋯	⋯	⋯	1
DSiF $\tilde{X}\,^1A'$							
CCSD(T)/aug-cc-pVQZ	1444	647	862	1403	638	847	Present
IR matrix	⋯	⋯	⋯	1387.4	638.4	833.4	18
Fitted HFF (calc.)[c]	1423.3	636.0	836.0	⋯	⋯	⋯	3
LIF hot bands	⋯	642.9(3)	⋯	⋯	642	⋯	3
Emissions ($\omega_i^{0''}$)[d]	1420.2(35)	642.21(50)	839.58(56)	1400.6	638.3	840.2	1
Observed (ω_i)[e]	1443.5(30)	648.7(10)	839.6(10)	⋯	⋯	⋯	1
Fitted HFF (calc.)[c]	1444.5	648.2	840.2	⋯	⋯	⋯	1

[a]Estimated uncertainties/errors in parentheses; see original works for details.
[b]K. J. Gregory and R. S. Grev (unpublished) quoted in Ref. 2.
[c]Harmonic force fields (HFF) with centrifugal distortion constants of the ground and excited states from gas phase analysis of the 0_0^0 band; see original works for details.
[d]Harmonic vibrational frequencies from the fitting of the observed band origins to the standard vibrational anharmonic expression of $G_0(\nu) = \omega_1^0\nu_1 + \omega_2^0\nu_2 + \omega_3^0\nu_3 + x_{11}^0\nu_2^2 + x_{22}^0\nu_2^2 + x_{12}^0\nu_1\nu_2$; see original work for detail.
[e]Force field refined $\omega_i = \omega_i^0 - x_{i1}^0 - (1/2)x_{i2}^0 - (1/2)x_{i3}^0$, where x_{ij} is the first order anharmonic term of the i and j modes. For the SiF stretching mode of HSiF, the harmonic frequency has assumed the fundamental value, because overtone levels in ν_3 were not observed. See original work for detail.

J. Chem. Phys., Vol. 120, No. 3, 15 January 2004

Simulated spectra of HSiF   1297

TABLE V. Computed and observed vibrational frequencies[a] (cm^{-1}) of the $\tilde{A}\ ^1A''$ state of HSiF and DSiF.

	ω_1(SiH)	ω_2(bend)	ω_3(SiF)	ν_1	ν_2	ν_3	Reference
HSiF $\tilde{A}\ ^1A'$							
CAS/MRCI/aug-cc-pVQZ	1829	603	873	1606	583	858	Present
CAS/TZ(2df,2pd)	1544	570	865	⋯	⋯	⋯	GG[b]
CCSD/aug-cc-pVTZ	1845	596	863	⋯	⋯	⋯	4[c]
LIF ($\omega_i^{0\prime}$)[d]	1547.8(27)	566.9(21)	858.6(25)	1547	558	857	2
LIF ($\omega_i^{0\prime}$)[e]	1546.95(9)	562.9(2)	861.77(9)	1547	558	857	3
Observed (ω_i')[f]	1815.6(13)	597.1(3)	867.8(5)	⋯	⋯	⋯	3
Fitted HFF (calc.)[g]	1836.3	590.2	870.8	⋯	⋯	⋯	3
DSiF $\tilde{A}\ ^1A'$							
CAS/MRCI/aug-cc-pVQZ	1319	451	869	1209	442	853	Present
LIF ($\omega_i^{0\prime}$)[e]	1241.8(7)	426.8(2)	859.6(4)	1174	430	854	3
Observed (ω_i')[f]	1322.4(8)	443.5(3)	867.2(5)	⋯	⋯	⋯	3
Fitted HFF (calc.)[g]	1321.2	442.4	866.9	⋯	⋯	⋯	3

[a]Estimated uncertainties/errors in parentheses; see original works for details.
[b]K. J. Gregory and R. S. Grev (unpublished), quoted in Ref. 2.
[c]Excited state calculation by the coupled cluster response theory (Ref. 4).
[d]Harmonic vibrational frequencies from the fitting of the observed band origins to the expression, $\bar{v} = T_{00} + \omega_1^{0\prime}\nu_1' + \omega_2^{0\prime}\nu_2' + \omega_3^{0\prime}\nu_3' + x_{22}^{0\prime}\nu_2'^2 + x_{12}^{0\prime}\nu_2'\nu_3' + x_{23}^{0\prime}\nu_2'\nu_3' + x_{13}^{0\prime}\nu_1'\nu_3'$; see original work for detail.
[e]Harmonic vibrational frequencies from the fitting of the observed band origins to the expression, $\bar{v} = T_{00} + \Sigma_{i=1}^3 \omega_i^{0\prime}\nu_i' + \Sigma_{i=1}^3\Sigma_{j\geqslant i}^3 x_{ij}'\nu_i'\nu_j' + \Sigma_{i=1}^3\Sigma_{j\geqslant i}^3\Sigma_{k\geqslant j}^3 x_{ijk}^{0\prime}\nu_i'\nu_j'\nu_k' - [\omega_2^{0\prime\prime} + x_{22}^{0\prime\prime}(\nu_2'')^2]$; see original work for detail.
[f]Force field refined $\omega_i = \omega_i^0 - x_{i1}^0 - (1/2)x_{i2}^0 - (1/2)x_{i3}^0$, where x_{ij} is the first order anharmonic term of the i and j modes. For HSiF, approximate anharmonicities and the product rule expression of isotopic substitution were used. See original work and also Ref. 1 for details.
[g]Harmonic force fields (HFFs) with centrifugal distortion constants of the ground and excited states from gas phase analysis of the 0_0^0 band; see original work for detail.

II, the vibrational labels according to the normal mode designations of these anharmonic vibrational wave functions may not be good quantum numbers, particularly for ν_2'' and ν_3''. In addition, ν_2'' and ν_3'' may not correspond to the bending and SiF stretching mode, respectively, as conventionally assumed (e.g., in HCJ01).[1] Nevertheless, for the sake of simplicity and ease of comparison with the vibrational assignments given in HCJ01,[1] we will still use the vibrational labels obtained in the way mentioned above and will not make a distinction between the vibrational designations used here and in HCJ01. It should be borne in mind that, for higher energy vibrational levels of the $\tilde{X}\ ^1A'$ state of HSiF, ν_2'' and ν_3'' may not be good quantum numbers and may not correspond to the bending and SiF stretching modes, respectively, as assumed in HCJ01, because of strong coupling. It is noted, however, that there is no such problem of strong mixing, as discussed, in the anharmonic vibrational wave functions of the $\tilde{X}\ ^1A'$ state of DSiF and their vibrational designations correspond to the DSi stretching, bending, and SiF stretching of the leading harmonic basis function.

Finally, a few points should be noted. First, the extent of mixing of the vibrational states within a combination manifold, as shown in the calculated anharmonic wave functions, is dependent on the closeness of the calculated energies of the vibrational levels within the manifold, which is dependent on the level of theory used to obtain the PEF of the $\tilde{X}\ ^1A'$ state. The difference between the computed fundamental frequencies of the bending and SiF stretching modes of 15 cm^{-1} is in reasonably good agreement with the corresponding experimental difference of 21 cm^{-1} reported in HCJ01[1] (see Table IV and later text), suggesting that the PEF of the $\tilde{X}\ ^1A'$ state should be reasonably reliable. In this connection, the calculated anharmonic wave functions reported

here should give a reasonably accurate description of the mixing. Second, since the experimental resolution of HCJ01[1] is not good enough to resolve some of these vibrational states within a combination manifold as discussed above, the uncertainties associated with the observed positions given in HCJ01 are probably larger than those quoted, because of the uncertainties associated with the assignments of overlapped vibrational components. Third, although a spectral resolution, which is able to resolve all the above-mentioned combination bands, can be used in the simulated spectra, a poorer resolution of 30 cm^{-1} FWHM has been used in order to make sensible comparison with the observed spectra.

B. Equilibrium geometrical parameters

The equilibrium geometrical parameters of both states of HSiF obtained from the PEFs are given in Table III together with available experimental and theoretical values for comparison. From Table III it can be seen that, compared to the reported calculations, the levels of calculation used in the present study are higher and hence the computed geometrical parameters obtained here can be considered as the most reliable theoretical values currently available for both the $\tilde{X}\ ^1A'$ and $\tilde{A}\ ^1A''$ states of HSiF. When the equilibrium HSi bond length and HSiF bond angle of the $\tilde{X}\ ^1A'$ state obtained from the CCSD(T)/aug-cc-pVQZ PEF are compared with the experimentally derived, estimated r_e^z values of HCJ01,[1] the agreement of within 0.001 Å and 0.2°, respectively, is excellent. However, the equilibrium SiF bond length obtained from the PEF of the $\tilde{X}\ ^1A'$ state is ~0.01 Å larger than the experimentally derived, estimated r_e^z value. Nevertheless, the CCSD(T)/aug-cc-pVQZ SiF value is, of all the computed values shown in Table III, the closest to the experimentally
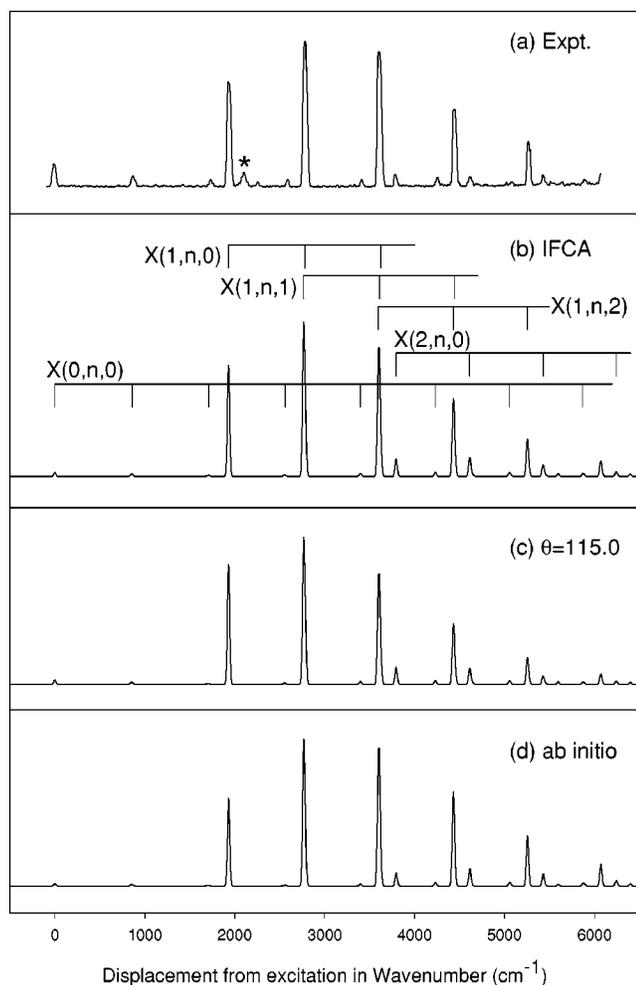
HSiF SVL A(1,0,0) Emission Spectra

(a) Expt.

(b) IFCA

X(1,n,0)

X(1,n,1)

X(1,n,2)

X(2,n,0)

X(0,n,0)

(c) θ=115.0

(d) ab initio

Displacement from excitation in Wavenumber (cm^{-1})

FIG. 1. Simulated and observed SVL $\tilde{A}(1,0,0)$ emission spectra of HSiF: (a) experimental spectrum from reference 1 (spectral feature due to impurity is marked with *; see original work); (b) simulated spectrum with $r_e(\text{SiF})$ = 1.597 Å, $r_e(\text{HSi})$ = 1.526 Å, and $\theta_e(\text{HSiF})$ = 116.0° [which give the best overall match between all simulated and observed spectra shown in Figs. 1, 3, 4, 5, and 6; the $\tilde{X} ^1A'$ state has its geometrical parameters fixed to $r_e(\text{SiF})$ = 1.603 Å, $r_e(\text{HSi})$ = 1.529 Å, and $\theta_e(\text{HSiF})$ = 96.6°, the estimated r_e^z values from HCJ01 (Ref. 1) for all the simulations carried out in this work; see text]; (c) simulated spectrum with $r_e(\text{SiF})$ = 1.597 Å, $r_e(\text{HSi})$ = 1.526 Å, and $\theta_e(\text{HSiF})$ = 115.0° (experimentally derived r_e geometrical parameters of the $\tilde{A} ^1A''$ state from Ref. 3, see Table V); and (d) simulated spectrum with $r_e(\text{SiF})$ = 1.6097 Å, $r_e(\text{HSi})$ = 1.5226 Å, and $\theta_e(\text{HSiF})$ = 116.9° (*ab initio* geometry change; see text).

derived value. The overestimation of the computed SiF bond length of the $\tilde{X} ^1A'$ state is most likely due to the neglect of core–core and core–valence correlation in all the reported calculations on HSiF, which includes of the second row element, Si (see for example, Ref. 17). However, the inclusion of core electrons in the correlation calculation will increase the total number of electrons to be correlated considerably, and also require a significantly larger polarized core–valence basis set. Such calculations are computationally extremely demanding.

For the $\tilde{A} ^1A''$ state, the equilibrium SiF bond length and HSiF bond angle obtained from the MRCI PEF are larger
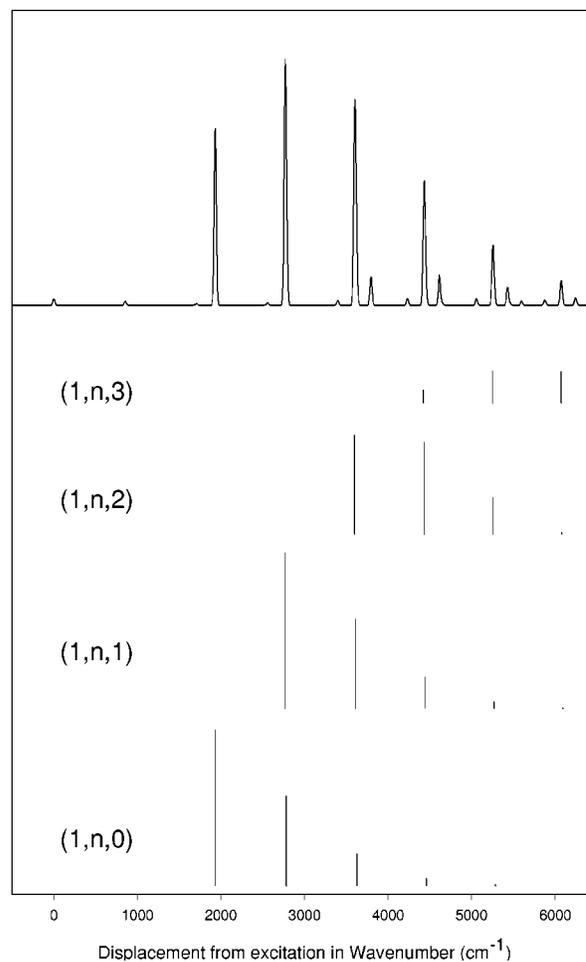
HSiF SVL A(1,0,0) Emission Spectra with FCF

(1,n,3)

(1,n,2)

(1,n,1)

(1,n,0)

Displacement from excitation in Wavenumber (cm^{-1})

FIG. 2. The simulated spectrum of the SVL $\tilde{A}(1,0,0)$ emission of HSiF, employing *ab initio* geometry change [same as Fig. 1(d)], and the calculated Franck–Condon factors (bar diagrams underneath the simulated spectrum) of the $\tilde{X}(1,n,0)$, $(1,n,1)$, $(1,n,2)$, and $(1,n,3)$ series, which contribute to the observed main vibrational progression assigned solely to the $\tilde{X}(1,n,0)$ series in Ref. 1 (see text).

than the experimentally derived equilibrium values of Ref. 3 by 0.02 Å and 1.7°, respectively, while the HSi bond length is smaller by 0.003 Å. The IFCA geometrical parameters derived for the $\tilde{A} ^1A''$ state will be discussed later, when the simulated spectra are compared with the observed spectra. It is just noted here that upon de-excitation from the $\tilde{A} ^1A''$ state to the $\tilde{X} ^1A'$ state, the equilibrium bond angle obtained from the PEFs decreases by nearly 20° in line with the experimentally derived values (see Table III). However, the changes in the HSi and SiF bond lengths obtained from the PEFs of the two states upon de-excitation from the $\tilde{A} ^1A''$ state to the $\tilde{X} ^1A'$ state are opposite in direction to those of the experimentally derived, estimated equilibrium r_e^z values. Nevertheless, in all cases, the magnitudes of the changes in bond lengths upon de-excitation are relatively small ($\leqslant 0.007$ Å) and the major geometry change upon de-excitation is in the bond angle. Perhaps the discrepancies between the changes in the computed and experimentally derived bond lengths upon de-excitation should not be surprising, because
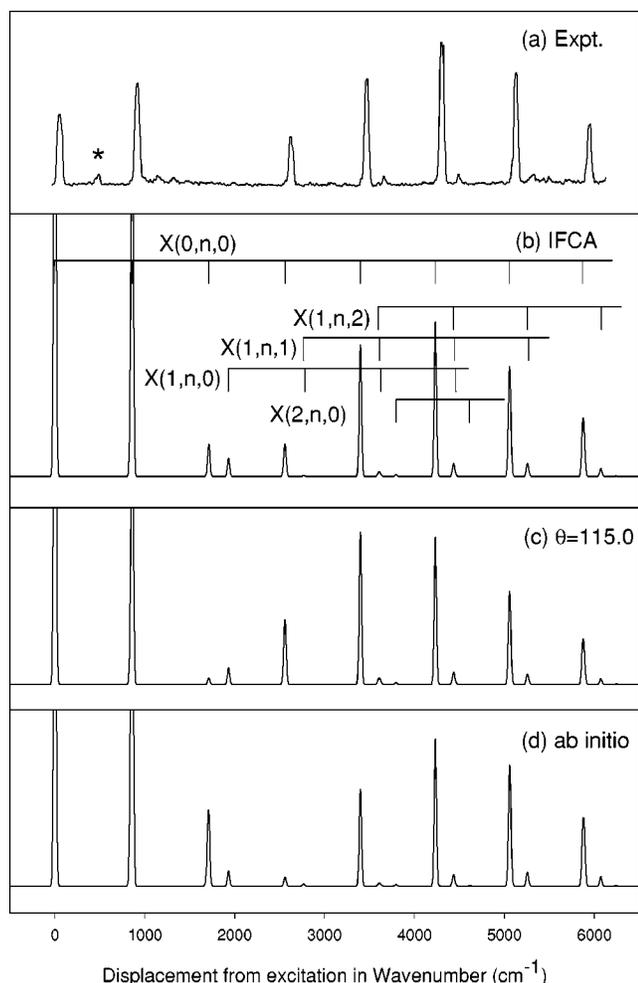
HSiF SVL A(0,1,0) Emission Spectra

FIG. 3. Simulated and observed SVL $\tilde{A}(0,1,0)$ emission spectra of HSiF: (a) experimental spectrum from Ref. 1 (spectral feature due to impurity is marked with *; see original work); (b) simulated spectrum with the IFCA geometrical parameters of $r_e(\text{SiF}) = 1.597$ Å, $r_e(\text{HSi}) = 1.526$ Å, and $\theta_e(\text{HSiF}) = 116.0°$ for the $\tilde{A}\,^1A''$ state (the best overall match; see text); (c) simulated spectrum with $r_e(\text{SiF}) = 1.597$ Å, $r_e(\text{HSi}) = 1.526$ Å, and $\theta_e(\text{HSiF}) = 115.0°$ (experimentally derived r_e geometrical parameters of the $\tilde{A}\,^1A''$ state from Ref. 3, see Table V); and (d) simulated spectrum with $r_e(\text{SiF}) = 1.6097$ Å, $r_e(\text{HSi}) = 1.5226$ Å, and $\theta_e(\text{HSiF}) = 116.9°$ (ab initio geometry change; see text).
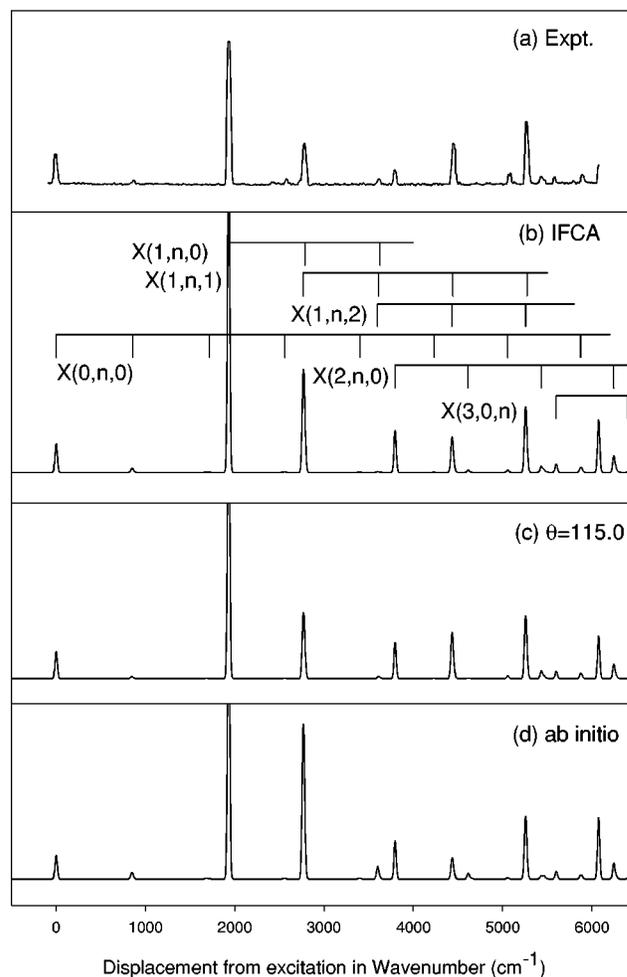
HSiF SVL A(1,1,0) Emission Spectra

FIG. 4. Simulated and observed SVL $\tilde{A}(1,1,0)$ emission spectra of HSiF; (a) experimental spectrum from Ref. 1; (b) simulated spectrum with $r_e(\text{SiF}) = 1.597$ Å, $r_e(\text{HSi}) = 1.526$ Å, and $\theta_e(\text{HSiF}) = 116.0°$ (the best overall match; see text); (c) simulated spectrum with $r_e(\text{SiF}) = 1.597$ Å, $r_e(\text{HSi}) = 1.526$ Å, and $\theta_e(\text{HSiF}) = 115.0°$ (experimentally derived r_e geometrical parameters of the $\tilde{A}\,^1A''$ state from Ref. 3, see Table V); and (d) simulated spectrum with $r_e(\text{SiF}) = 1.6097$ Å, $r_e(\text{HSi}) = 1.5226$ Å, and $\theta_e(\text{HSiF}) = 116.9°$ (ab initio geometry change; see text).

different correlation methods were employed to obtain the PEFs of the two electronic states. However, when the computed CCSD/aug-cc-pVTZ equilibrium HSi bond lengths of the two states reported in Ref. 4 (the excited state geometry was obtained by the coupled cluster response method) are compared with the corresponding experimentally derived, estimated r_e^z values, the changes upon de-excitation are also opposite in direction. The above considerations suggest that obtaining reliable geometrical parameters for the excited state of HSiF is theoretically very demanding in terms of the level of calculation, as expected. In addition, it should be noted that the uncertainties associated with the experimentally derived geometrical parameters of the $\tilde{A}\,^1A''$ state are also larger than those of the $\tilde{X}\,^1A'$ state. In particular, the

uncertainty in the experimentally derived HSi bond length of the $\tilde{A}\,^1A''$ state (equilibrium r_e in Table III) of 0.014 Å quoted in Ref. 3 is rather large, and the difference between the experimentally derived, equilibrium r_e, and estimated r_e^z values of HSi of the $\tilde{A}\,^1A''$ state is 0.01 Å, which is also quite large (see Table III). The changes in the equilibrium geometrical parameters upon de-excitation will be further discussed, when the IFCA geometry of the $\tilde{A}\,^1A''$ state is considered.

C. Vibrational frequencies

The computed harmonic and fundamental vibrational frequencies (listed in wave number units) obtained from the PEFs of the two electronic states of HSiF (and DSiF), are given in Tables IV and V, respectively, together with available theoretical and experimental values. First, since no ab

DSiF SVL A(0,0,0) Emission Spectra

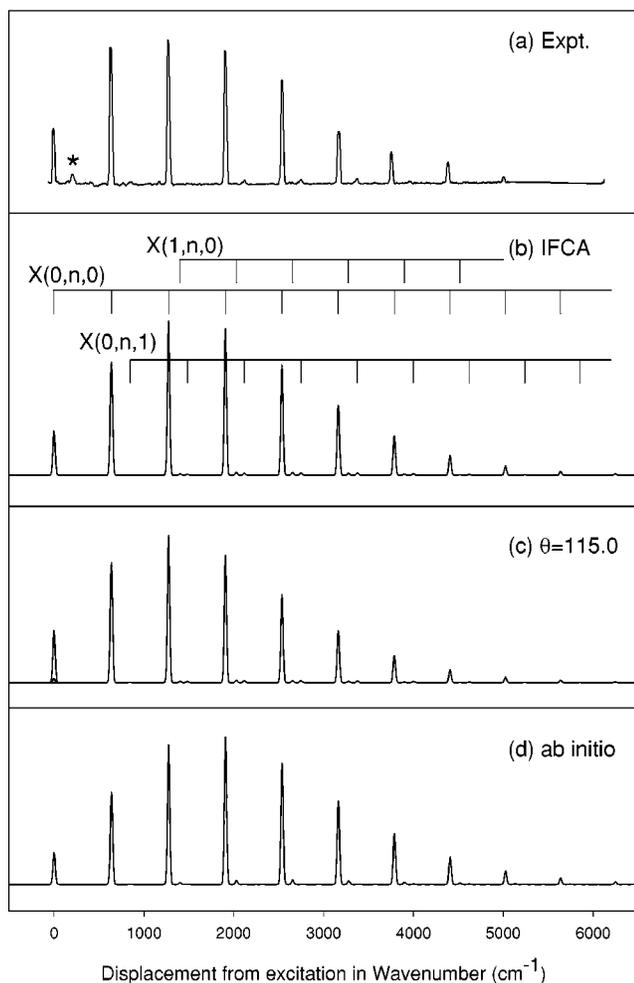## DSiF SVL A(0,1,0) Emission Spectra

FIG. 5. Simulated and observed SVL $\tilde{A}(0,0,0)$ emission spectra of DSiF: (a) experimental spectrum from Ref. 1 (spectral feature due to impurity is marked with *; see original work); (b) simulated spectrum with $r_e(\text{SiF})$ = 1.597 Å, $r_e(\text{DSi})$ = 1.526 Å, and $\theta_e(\text{DSiF})$ = 116.0° (the best overall match; see text); (c) simulated spectrum with $r_e(\text{SiF})$ = 1.597 Å, $r_e(\text{HSi})$ = 1.526 Å, and $\theta_e(\text{HSiF})$ = 115.0° (experimentally derived r_e geometrical parameters of the $\tilde{A}\,^1A''$ state from Ref. 3, see Table V); and (d) simulated spectrum with $r_e(\text{SiF})$ = 1.6097 Å, $r_e(\text{HSi})$ = 1.5226 Å, and $\theta_e(\text{HSiF})$ = 116.9° (*ab initio* geometry change; see text).
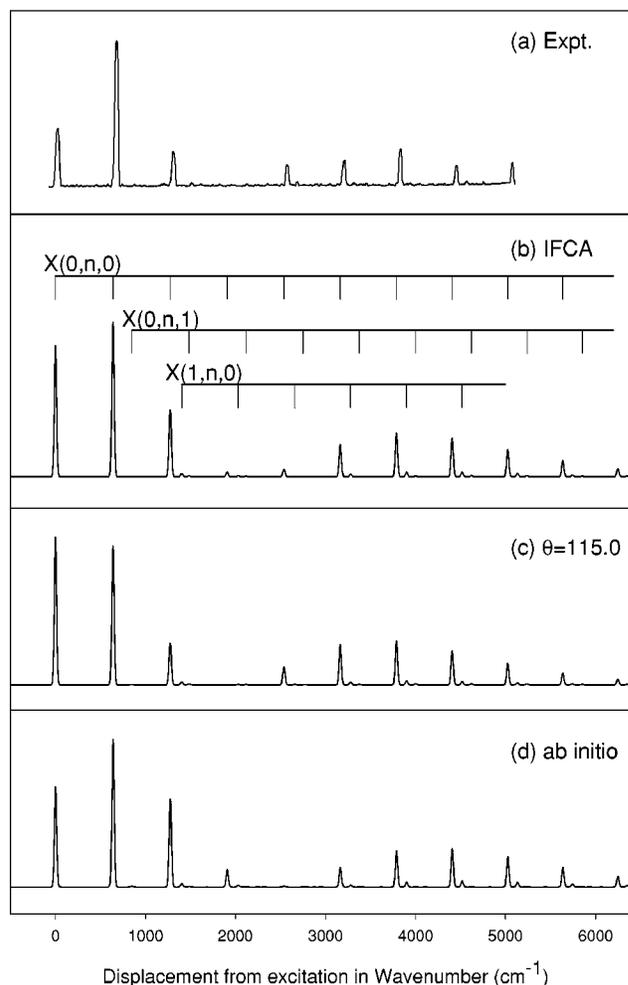
FIG. 6. Simulated and observed SVL $\tilde{A}(0,1,0)$ emission spectra of DSiF: (a) experimental spectrum from Ref. 1, (b) simulated spectrum with $r_e(\text{SiF})$ = 1.597 Å, $r_e(\text{DSi})$ = 1.526 Å, and $\theta_e(\text{DSiF})$ = 116.0° (the best overall match; see text); (c) simulated spectrum with $r_e(\text{SiF})$ = 1.597 Å, $r_e(\text{HSi})$ = 1.526 Å, and $\theta_e(\text{HSiF})$ = 115.0° (experimentally derived r_e geometrical parameters of the $\tilde{A}\,^1A''$ state from Ref. 3, see Table V); and (d) simulated spectrum with $r_e(\text{SiF})$ = 1.6097 Å, $r_e(\text{HSi})$ = 1.5226 Å, and $\theta_e(\text{HSiF})$ = 116.9° (*ab initio* geometry change; see text).

initio fundamental vibrational frequencies have been calculated prior to the present study, measured fundamental frequencies can be compared directly only with the calculated fundamental frequencies reported here. Second, from Tables IV and V, the most obvious observation is the large differences between the computed harmonic and fundamental vibrational frequencies of the HSi/DSi stretching mode, particularly for the $\tilde{A}\,^1A''$ state (of >200/100 cm^{-1}, respectively), as expected and mentioned above. It seems clear that, previous experimentally derived harmonic frequencies of the HSi/DSi stretching mode of the $\tilde{A}\,^1A''$ state (~1547/1242 cm^{-1}), which are close to the observed fundamental values (1547/1174 cm^{-1}; LIF $\omega_i^{0\prime}$ values from Refs. 2 and 3 in Table V), are in error. This was mainly because of the lack of observed higher energy vibrational components in

the HSi/DSi progressions of the LIF spectra. In addition, the computed CAS/TZ(2df,2pd) harmonic HSi stretching frequency of the $\tilde{A}\,^1A''$ state of HSiF of 1544 cm^{-1} by Gregory and Grev (see Table V; unpublished, quoted in Ref. 2) might also have misled the vibrational analyses of Refs. 2 and 3. It is clear that the CAS/TZ(2df,2dp) harmonic HSi stretching frequency of the $\tilde{A}\,^1A''$ state (1544 cm^{-1}) is significantly smaller than the corresponding computed harmonic HSi stretching frequencies obtained at the CCSD/aug-cc-pVTZ level by Christiansen *et al.*[4] (1845 cm^{-1}) and at the CASSCF/MRCI/aug-cc-pVQZ level in the present study (1829 cm^{-1}), and also the force-field refined values of 1816 and 1836 cm^{-1} given in Ref. 3 [observed (ω_i') and fitted HFF (calc.) values in Table V]. Therefore, it seems conclusive that the CAS/TZ(2df,2dp) level, which lacks dynamic electron correlation, is inadequate for the potential energy

surface of the $\tilde{A}\,^1A''$ state. The harmonic HSi/DSi vibrational frequencies obtained from the CASSCF/MRCI/aug-c-pVQZ PEF of the $\tilde{A}\,^1A''$ state in the present study agrees very well with experimentally derived harmonic values where force field refinements have been carried out (observed ω_i' and fitted HFF values in Table V), supporting the validity of the force field refinements carried out in Ref. 3 (and also Ref. 1).

Third, comparing the computed and experimental vibrational frequencies in detail, the harmonic and fundamental vibrational frequencies of the HSi/DSi stretching and bending modes obtained from the variational calculations of the $\tilde{X}\,^1A'$ state of HSiF/DSiF agree very well with the latest experimentally derived (force field refined as discussed above) or measured values of HCJ01 (to within ~ 2 cm^{-1}; see Table IV). The agreement between the theoretical and experimental values of the SiF stretching frequencies of HSiF/DSiF is less favorable. This is not surprising, because the computed SiF bond length of the $\tilde{X}\,^1A'$ state is ~ 0.01 Å larger than the experimentally derived value, as discussed above. Nevertheless, the largest discrepancy for the harmonic frequency is 22 cm^{-1} and that for the fundamental frequency is only 7 cm^{-1}, which can be considered as reasonably small.

Finally, for the $\tilde{A}\,^1A''$ state, the agreements between the calculated and experimentally derived (force field refined as discussed above) or measured values of the SiF stretching harmonic and fundamental frequencies of both HSiF and DSiF are very good ($\leqslant \sim 3$ cm^{-1}; see Table V). However, the discrepancies for the fundamental HSi/DSi stretching and the bend frequencies are significantly larger. The largest difference is that between the calculated and observed HSi stretching fundamental frequencies, which is 59 cm^{-1}. We attempted to improve the agreement by extending the ranges of the *ab initio* energy scans for the PEF of the $\tilde{A}\,^1A''$ state and enlarging the size of the harmonic basis functions employed in the variational calculation, but found that no significant improvement could be obtained. It is therefore concluded that the PEF of the $\tilde{A}\,^1A''$ state probably requires a higher level of calculation in terms of both the correlation method and the basis set used, in order to obtain a better agreement between the calculated and observed HSi/DSi stretching fundamental frequencies of the $\tilde{A}\,^1A''$ state of HSiF/DSiF. In addition, core–valence correlation, which has been ignored in the *ab initio* calculations, as discussed in the previous subsection on the calculation of reliable geometrical parameters for this type of system, is also likely to be important for reliable vibrational frequency calculations.

D. Spectral simulation

The simulated SVL emission spectra of HSiF and DSiF are compared with the corresponding observed spectra in Figs. 1, 3, 4, 5, and 6 for the $\tilde{A}(1,0,0)$, $\tilde{A}(0,1,0)$, and $\tilde{A}(1,1,0)$ SVL emissions of HSiF, and the $\tilde{A}(0,0,0)$ and $\tilde{A}(0,1,0)$ SVL emissions of DSiF, respectively. The top spectrum labeled (a) in each figure is the observed spectrum from HCJ01.[1] In all figures, the simulated spectra labeled (b), (c), and (d), below (a), have the following geometrical param-

eters of the $\tilde{A}\,^1A''$ state [in all simulated spectra, the $\tilde{X}\,^1A'$ state has its geometrical parameters fixed to $r_e(\mathrm{SiF})$ = 1.603 Å, $r_e(\mathrm{HSi})$ = 1.529 Å, and $\theta_e(\mathrm{HSiF})$ = 96.6°, the estimated r_e^z values from HCJ01;[1] see Table 3]:
(b) $r_e(\mathrm{SiF})$ = 1.597 Å, $r_e(\mathrm{HSi})$ = 1.526 Å, and $\theta_e(\mathrm{HSiF})$ = 116.0° (the IFCA geometry with the best overall match; see later text);
(c) $r_e(\mathrm{SiF})$ = 1.597 Å, $r_e(\mathrm{HSi})$ = 1.526 Å, and $\theta_e(\mathrm{HSiF})$ = 115.0° (experimentally derived r_e geometrical parameters from Ref. 3); and
(d) $r_e(\mathrm{SiF})$ = 1.6097 Å, $r_e(\mathrm{HSi})$ = 1.5226 Å, and $\theta_e(\mathrm{HSiF})$ = 116.9° (*ab initio* geometry change).

When the simulated and observed spectra are compared, the following points should be noted. First, some peaks in some of the observed spectra are due to impurities as noted in HCJ01[1] [marked with* in the observed spectra shown in Figs. 1(a), 3(a), and 5(a)]. Second, the relative intensity of the vibrational component at the excitation energy in an observed emission spectrum is expected to be stronger than the intensity given by its FC factor, because of stimulated emission and scattered light. Third, the reported dispersed fluorescence spectra of DSiF from HCJ01[1] [Figs. 5(a) and 6(a); see original work] were uncorrected for the wavelength dependence of the detector efficiency. Consequently, only qualitative comparisons between the simulated and observed spectra of DSiF can be made. Finally, the wave number scale of each figure is displacement from the laser excitation line, giving a direct measure of the ground electronic state vibrational energy, as used in HCJ01.[1]

1. The $\tilde{A}(1,0,0)$ SVL emission of HSiF

The simulated and observed $\tilde{A}(1,0,0)$ SVL emission spectra in Fig. 1 are considered first, because the match between the simulated spectrum (d), employing the *ab initio* geometry change, and the observed spectrum (a) is excellent, with even the very weak features in the vibrational progressions of $\tilde{X}(0,\nu_2'',0)$ and $\tilde{X}(2,\nu_2'',0)$ being present in the simulated spectrum. Such a good agreement between theory and experiment suggests that the PEFs and the *ab initio* geometry change employed in obtaining the simulated spectrum should be reasonably reliable. Comparing the simulated spectrum (c), which employs the experimentally derived geometrical parameters of the $\tilde{A}\,^1A''$ state, with the observed spectrum (a), the agreement is slightly worse in the higher energy members of the main progression assigned to the $\tilde{X}(1,\nu_2'',0)$ series in HCJ01[1] than the agreement between the simulated spectrum (d), employing the *ab initio* geometry change, and the observed spectrum. The major difference between the geometry of the $\tilde{A}\,^1A''$ state used in the simulations of spectra (c) and (d) is in the bond angle, as the major vibrational progressions observed upon de-excitation involve mainly the bending mode. This follows from the fact that the major geometry change upon de-excitation is in the bond angle, as discussed.

Regarding the bond length changes upon de-excitation, it should be noted that FC factors depend on the magnitude of relative changes of the geometrical parameters in the electronic transition, and comparisons between simulated and

observed spectra cannot indicate the directions of the changes (i.e., whether there is a small increase or decrease) in the geometrical parameters. Previously, in the IFCA procedure, the systematic variation in the geometrical parameters of one of the two electronic states involved in the electronic transition, which did not have its geometry derived experimentally, was usually based on the geometry change obtained from *ab initio* calculations (see Refs. 5, 6, and 7, and references therein). However, in the case of HSiF, experimentally derived geometrical parameters are available for both states, but their directions of change in the HSi and SiF bond lengths upon de-excitation are exactly opposite to those of the corresponding *ab initio* geometry change, as discussed above. In the IFCA procedure, it was found that the effects of bond length changes upon de-excitation on the simulated spectrum are smaller than those of bond angle change, and the IFCA procedure carried out was unable to determine unambiguously which directions of change in these bond lengths are more reliable from comparisons between simulated and observed spectra. This will be further discussed when the SVL emissions of DSiF are considered. At the moment, it is assumed that the experimentally derived bond lengths from the Clouthier group[3] are more reliable, until further, higher level *ab initio* calculations are available (see next section) and the HSiF angle in the $\tilde{A}\,^1A''$ state is changed to fit the observed SVL emission spectra.

It has been mentioned above that some higher energy vibrational levels of the $\tilde{X}\,^1A'$ states are calculated to be close in energy, and the corresponding vibrational components which appear in both the simulated and observed spectra are unresolved. Nevertheless, from our computed anharmonic FC factors, the observed main vibrational progression assigned solely to the $\tilde{X}(1,\nu_2'',0)$ series in HCJ01,[1] has actually significant contributions from the $\tilde{X}(1,\nu_2'',1)$, $(1,\nu_2'',2)$, and $(1,\nu_2'',3)$ series, as shown in Fig. 2. Specifically, the first vibrational component of the observed main series observed at 1932 cm^{-1} is solely due to the SVL emission to the $\tilde{X}(1,0,0)$ anharmonic vibrational level. The second component observed at 2771 cm^{-1} has strong contributions from the SVL emissions to both the $\tilde{X}(1,0,1)$ and $(1,1,0)$ levels, while from the third component observed at 3606 cm^{-1} onwards, there are contributions from the vibrational series of $\tilde{X}(1,\nu_2'',0)$, $(1,\nu_2'',1)$, $(1,\nu_2'',2)$, etc. Based on the computed FC factors obtained in this work, some of the vibrational assignments given in HCJ01[1] should be revised.

Summing up, the most important conclusion from the excellent agreement between the simulated and observed $\tilde{A}(1,0,0)$ SVL emission spectra of HSiF is that the explicit inclusion of anharmonicity in the FC factor calculations, as carried out in the present investigation, has answered, at least partially, the request of the experimental study of HCJ01.[1] In this connection, it can be concluded that the *ab initio* calculations and PEFs employed to calculate FC factors between the two electronic states of HSiF are reasonably reliable for simulating other SVL emissions of HSiF/DSiF to be discussed below. From the detailed comparisons between simulated and observed spectra of the $\tilde{A}(1,0,0)$ SVL emission in the IFCA procedure, we are unable to derive the bond

lengths of the upper state unambiguously. However, a larger equilibrium bond angle of 116.9° (from the *ab initio* geometry change) of the $\tilde{A}\,^1A''$ state is preferred to the smaller experimentally derived bond angle of 115.0°. This will be further discussed, when other SVL emissions are considered. Finally, the calculated FC factors and simulated spectra obtained in this work suggest that the observed main vibrational progression assigned to the $\tilde{X}(1,\nu_2'',0)$ series by HCJ01[1] actually also has significant contributions from the overlapping $\tilde{X}(1,\nu_2'',1)$, $(1,\nu_2'',2)$, and $(1,\nu_2'',3)$ series, particularly for the higher energy members of the observed main vibrational progression.

2. The $\tilde{A}(0,1,0)$ SVL emission of HSiF

When the simulated and observed $\tilde{A}(0,1,0)$ SVL emission spectra in Fig. 3 are considered, the agreement between the simulated spectrum (d), employing the *ab initio* geometry change, and the observed spectrum (a) is reasonably good for the observed main $\tilde{X}(0,\nu_2'',0)$ series, with $\nu_2'' \geq 4$, and also for the weak feature assigned to the start of the $\tilde{X}(1,\nu_2'',0)$ series in HCJ01.[1] However, for the vibrational components with $\nu_2'' \leq 3$ in the $\tilde{X}(0,\nu_2'',0)$ series, the agreement is poor, particularly for the $\tilde{X}(0,0,0)$ and $(0,1,0)$ peaks. The computed relative intensities of these two vibrational components are a few times stronger than those observed. Employing the experimentally derived geometrical parameters of the $\tilde{A}\,^1A''$ state gives the spectrum shown in Fig. 3(c). In both simulated spectra in Figs. 3(c) and 3(d), however, the simulated relative intensities of the $\tilde{X}(0,0,0)$ and $(0,1,0)$ components are much stronger than those observed. In the IFCA procedure of systematically varying the upper state geometrical parameters, it was found that it was impossible to obtain an overall match between simulated spectra and the full experimental spectrum of the $\tilde{A}(0,1,0)$ SVL emission with reasonable geometry changes based on the experimentally derived and/or *ab initio* geometries (see Ref. 7 for a discussion of why excessive variations of the geometrical parameters in the IFCA procedure are undesirable). It is noted that the theoretical model employed in the FC simulation of the present study has assumed the variation of electronic transition moment over a spectral band to be constant and this may be a cause of the discrepancies between the simulated and observed SVL emission spectra. However, the variation of electronic transition moment over a spectral band is expected to be gradual, except when an avoided crossing, where the electronic configuration of the electronic energy surface changes drastically, is present in the FC region of the electronic transition. From the computed T_1 diagnostics in the CCSD(T) calculations on the $\tilde{X}\,^1A'$ state and the calculated MRCI wave functions of the $\tilde{A}\,^1A''$ state, it is clear that there is no other electronic states nearby. In this connection, it is almost certain that the large discrepancies between the calculated and observed relative intensities of the $\tilde{X}(0,0,0)$ and $(0,1,0)$ vibrational components mentioned above cannot be due to

the neglect of the variation of electronic transition moment in the theoretical model employed to obtain the simulated spectra.

In view of the excellent agreement between the simulated and observed spectra of the $\tilde{A}(1,0,0)$ SVL emission, as discussed above, it is concluded that the simulated $\tilde{A}(0,1,0)$ SVL emission spectra shown in Fig. 3 should be reasonably reliable, and hence the true relative intensities of the $\tilde{X}(0,0,0)$ and $(0,1,0)$ vibrational components in the $\tilde{A}(0,1,0)$ SVL emission are most likely stronger than shown in the reported spectrum of HCJ01.[1] We speculate that the reduction of the observed relative intensities of these two vibrational components in the reported spectrum of HCJ01, which are predicted to be very intense, is possibly due to signal saturation of the detector, and the nonobservation of two weaker components at about ~1800 cm^{-1} relative to the excitation line is probably because of an experimental problem, such as this part of the spectrum being recorded with a lower detector gain relative to that used for the rest of the spectrum.

Ignoring the $\tilde{X}(0,0,0)$ and $(0,1,0)$ vibrational components in the $\tilde{A}(0,1,0)$ SVL emission spectrum, the simulated spectrum of the $\tilde{A}(0,1,0)$ SVL emission obtained with the *ab initio* geometry change [Fig. 3(d)] appears to agree slightly better with the observed spectrum [Fig. 3(a)] than that obtained by employing the experimentally derived geometry of the $\tilde{A}\,^1A''$ state [Fig. 3(c)] in the spectral region of >3000 cm^{-1}. This conclusion from comparisons between simulated and observed spectra of the $\tilde{A}(0,1,0)$ SVL emission is similar to that of the $\tilde{A}(1,0,0)$ SVL emission discussed above.

Finally, according to the calculated anharmonic FC factors, the observed weak vibrational progression assigned to the $\tilde{X}(1,\nu''_2,0)$ series by HCJ01[1] are due to the overlapping $\tilde{X}(1,\nu''_2,0)$, $(1,\nu''_2,1)$, and $(1,\nu''_2,2)$ series [see the vibrational designations given in Fig. 3(b)], similar to the main vibrational progression observed in the SVL $\tilde{A}(1,0,0)$ emission, as discussed above.

3. The $\tilde{A}(1,1,0)$ SVL emission of HSiF

Considering the $\tilde{A}(1,1,0)$ emission in Fig. 4, first, similar to the $\tilde{A}(0,1,0)$ emission discussed above, the general match between the simulated spectra of Figs. 4(c) and 4(d), and the observed spectra of Fig. 4(a) is reasonably good, with the exceptions of the $\tilde{X}(1,0,0)$ and, to a lesser extent, $\tilde{X}(1,1,0)$ vibrational components. The simulated relative intensities of these two vibrational components are considerably stronger than the observed relative intensities. It seems almost certain that the observed relative intensities of these two vibrational components reported in HCJ01[1] have suffered from an experimental problem, such as detector signal saturation, similar to the cases of the $\tilde{X}(0,0,0)$ and $(0,1,0)$ components in the observed $\tilde{A}(0,1,0)$ emission spectrum discussed above.

Apart from the $\tilde{X}(1,0,0)$ and $(1,1,0)$ vibrational components, the simulated spectrum (c) in Fig. 4, obtained employing the experimentally derived geometrical parameters of the

$\tilde{A}\,^1A''$ state, appears to match the observed spectrum [Fig. 4(a)] slightly better than the simulated spectrum with the *ab initio* geometry change [Fig. 4(d)] in the 3500–4700 cm^{-1} region. Specifically, a smaller bond angle of 115.0° gives simulated relative intensities of the vibrational components at 3788 and 4443 cm^{-1} [assigned to $\tilde{X}(2,0,0)$ and $(1,3,0)$ in HCJ01], which agree slightly better with the observed relative intensities, than those obtained with a larger bond angle of 116.9°. This is just the opposite of the conclusion reached from the comparisons between simulated and observed spectra discussed above for the $\tilde{A}(1,0,0)$ and $\tilde{A}(0,1,0)$ SVL emissions. In view of these differences in fitted bond angle, a bond angle of 116.0°, an intermediate value between the experimentally derived and *ab initio* values, has been employed as a compromise, giving spectra (b) in Figs. 1, 3, 4, 5, and 6. The upper state IFCA bond angle of 116.0° may be considered as the bond angle, which gives the best overall match between simulated and observed spectra for all the reported SVL emissions of HSiF (and DSiF; see next subsection) with the *ab initio* PEFs calculated in this work.

Finally, similar to the $\tilde{A}(0,0,0)$ and $\tilde{A}(0,1,0)$ SVL emissions of HSiF discussed above, the higher energy members of the vibrational progression observed in the $\tilde{A}(1,1,0)$ SVL emission spectrum, assigned to the $\tilde{X}(1,\nu''_2,0)$ series by HCJ01,[1] are due to the overlapping $\tilde{X}(1,\nu''_2,0)$, $(1,\nu''_2,1)$, $(1,\nu''_2,2)$, and $(1,\nu''_2,3)$ series based on the calculated FC factors.

4. The $\tilde{A}(0,0,0)$ and $\tilde{A}(0,1,0)$ SVL emissions of DSiF

Regarding the $\tilde{A}(0,0,0)$ and $\tilde{A}(0,1,0)$ SVL emissions of DSiF, the simulated and observed spectra are compared in Figs. 5 and 6, respectively. In view of the fact that the experimental spectra [Figs. 5(a) and 6(a)] have not been corrected for the wavelength dependence of the detector efficiency as mentioned earlier, it can be concluded that the matches between the simulated and observed SVL emission spectra of DSiF shown in Figs. 5 and 6 are reasonably satisfactory. This supports the conclusion that the *ab initio* PEFs and the geometry changes upon de-excitation employed in simulating the SVL emission spectra reported in this work should be reasonably reliable. However, it is not possible to decide on the best IFCA geometry of the $\tilde{A}\,^1A''$ state from the comparisons between simulated and observed SVL emission spectra of DSiF, because of the uncertainties associated with the relative intensities of each vibrational component of the observed spectra due to the wavelength dependence of the detector efficiency. Nevertheless, it can been seen that the weak $\tilde{X}(1,\nu''_2,0)$ series in the simulated spectra of the SVL $\tilde{A}(0,0,0)$ emission of DSiF [Figs. 5(b), 5(c), and 5(d)] is not observed in the experimental spectrum [Fig. 5(a)]. In the IFCA procedure, it was found that a significantly smaller $r_e(\text{HSi})$ value (of $\leqslant 1.510$ Å) for the $\tilde{A}\,^1A''$ state than those used to obtain the simulated spectra shown in Fig. 5 is required, in order to reduce the relative intensity of the $\tilde{X}(1,\nu''_2,0)$ series in the simulated spectrum to an extent that it matches the observed spectrum. This smaller $r_e(\text{HSi})$ value

of 1.510 Å, which is near the lower limit of the uncertainty of the experimentally derived r_e value of 1.526 ± 0.014 Å given in Ref. 3, suggests that the true value is probably towards the lower end of the experimentally derived value. It is noted that employing a smaller $r_e(\text{HSi})$ (e.g., 1.510 Å) for the $\tilde{A}\,^1A''$ state in the IFCA simulation does not change the relative intensities of the main vibrational features significantly in the simulated spectra of all the SVL emissions considered here, because the main vibrational progressions observed in these spectra are essentially bending series, as mentioned above. With this smaller value of $r_e(\text{HSi})$ for the $\tilde{A}\,^1A''$ state, small improvements of the matches between the simulated and observed spectra were found for the SVL $\tilde{A}(0,0,0)$ emission of DSiF, regarding the $\tilde{X}(1,\nu_2'',0)$ series discussed, and for the SVL $\tilde{A}(1,1,0)$ emission of HSiF in the 3700–4500 cm^{-1} region.

IV. CONCLUDING REMARKS

In response to the request of HCJ01,[1] *ab initio* PEFs of the $\tilde{X}\,^1A'$, and $\tilde{A}\,^1A''$ states of HSiF, anharmonic vibrational wave functions and energies of both electronic states of HSiF and DSiF, and FC factors with the explicit inclusion of anharmonicity between the two electronic states have been calculated. It is pleasing to conclude that simulated emission spectra including anharmonicity obtained in the present study match the observed $\tilde{A}\,^1A''(1,0,0)\rightarrow\tilde{X}\,^1A'$ emission spectrum of HSiF published in HCJ01 very well. Anharmonicity is indeed important in FC simulations of the observed SVL emission spectra of HSiF and DSiF, as suggested in HCJ01. In addition, comparisons between simulated and observed $\tilde{A}(0,1,0)$ and $(1,1,0)$ SVL emission spectra of HSiF suggest that some vibrational components, which are predicted to have strong relative intensities, but are observed to be significantly weaker than predicted, have suffered from intensity reduction due to some experimental problems, such as detector signal saturation and/or part of the spectrum being recorded with a lower detector gain. The reasonably good matches between the simulated and observed $\tilde{A}(0,0,0)$ and $(0,1,0)$ SVL emission spectra of DSiF also support the above conclusions.

In spite of the improvement of FC simulations by including anharmonicity in this work, it appears that there are still some inadequacies in the present theoretical approach. We are unable to find an IFCA geometry of the $\tilde{A}\,^1A''$ state of HSiF, which would give simulated spectra, which match all the observed SVL emission spectra of HSiF considered, to the same level of agreement. In view of the relatively large difference (of ~50 cm^{-1}) between the computed fundamental HSi stretching frequencies obtained from the CASSCF/MRCI/aug-cc-pVQZ PEF of this work and the corresponding measured value from Refs. 2 and 3 (see Table V), it appears that the level of theory used in obtaining the *ab initio* PEFs of the $\tilde{A}\,^1A''$ state of HSiF is probably inadequate for regions far away from the equilibrium position. In this connection, the simulated spectra of the $\tilde{A}(1,0,0)$ and $(0,1,0)$ SVL emissions would be expected to be slightly more reliable than the simulated spectrum of the $\tilde{A}(1,1,0)$ SVL emission, which

emits from a vibrational level of higher energy in the upper electronic state than the former two emissions. This leads to the conclusion that the larger bond angle of 116.9° of the $\tilde{A}\,^1A''$ state (based on *ab initio* geometry change) would be preferred, based on spectral simulation, to the experimentally derived r_e bond angle of 115.0°, and hence this casts doubt on the reliability of the latter. In view of the above considerations, further theoretical and experimental investigations would be required to establish the equilibrium geometry of the $\tilde{A}\,^1A''$ state of HSiF on a firmer basis. On the theoretical side, higher level *ab initio* calculations in terms of higher order electron correlation and a larger basis size are required to obtain a more reliable PEF of the $\tilde{A}\,^1A''$ state, and hence also a more accurate fundamental HSi stretching frequency and simulated emission spectra. In addition, in the comparison between the calculated and experimentally derived geometrical parameters of the $\tilde{X}\,^1A'$ state of HSiF, we have noted that the inclusion of core electrons in the correlation treatment of the *ab initio* calculations could be important to give a more reliable computed SiF bond length of the $\tilde{X}\,^1A'$ state. These suggested improvements in the level of *ab initio* calculations will lead to significantly more demanding calculations than presently carried out. Nevertheless, despite these inadequacies in the present theoretical approach and the inability of determining unambiguously the equilibrium geometry of the $\tilde{A}\,^1A''$ state of HSiF from the IFCA procedure, the major vibrational features of the simulated spectra reported in this investigation with the explicit inclusion of anharmonicity match reasonably well with those observed, and the computed anharmonic FC factors lead to a vibrational assignment of all the main observed features in the SVL emission spectra, which revises slightly the earlier assignment of Ref. 1, and provides more detail, particularly with respect to overlapping bands.

[1] D. A. Hostutler, D. J. Clouthier, and R. H. Judge, J. Chem. Phys. **114**, 10728 (2001).

[2] W. W. Harper, J. Karolczak, D. J. Clouthier, and S. C. Ross, J. Chem. Phys. **103**, 883 (1995).

[3] W. W. Harper, D. A. Hostutler, and D. J. Clouthier, J. Chem. Phys. **106**, 4367 (1997).

[4] O. Christiansen, T. A. Ruden, K. Ruud, and T. Helgaker, J. Chem. Phys. **116**, 8334 (2002).

[5] F.-T. Chau, J. M. Dyke, E. P. F. Lee, and D. K. W. Mok, J. Chem. Phys. **115**, 5816 (2001).

[6] D. C. Wang, F.-T. Chau, D. K. W. Mok, E. P. F. Lee, L. Beeching, J. S. Ogden, and J. M. Dyke, J. Chem. Phys. **114**, 10682 (2001).

[7] F. T. Chau, J. M. Dyke, E. P. F. Lee, and D. K. W. Mok, J. Chem. Phys. **118**, 4025 (2003).

[8] C. Hampel, K. Peterson, and H.-J. Werner, Chem. Phys. Lett. **190**, 1 (1992).

[9] J. D. Watts, J. Gauss, and R. J. Bartlett, J. Chem. Phys. **98**, 8718 (1993).

[10] H.-J. Werner and P. J. Knowles, J. Chem. Phys. **82**, 5053 (1985).

[11] H.-J. Werner and P. J. Knowles, J. Chem. Phys. **89**, 5803 (1988).

[12] D. E. Woon and T. H. Dunning, Jr., J. Chem. Phys. **98**, 1358 (1993).

[13] MOLPRO is a package of *ab initio* programs written by H.-J. Werner and P. J. Knowles; with contributions from J. Almlöf *et al.*

[14] S. Carter and N. C. Handy, J. Chem. Phys. **87**, 4294 (1987).

[15] J. K. G. Watson, Mol. Phys. **15**, 479 (1968).

[16] J. K. G. Watson, Mol. Phys. **19**, 465 (1970).

[17] D. Feller, K. A. Peterson, W. A. de Jong, and D. A. Dixon, J. Chem. Phys. **118**, 3510 (2003).

[18] Z. K. Ismail, L. Fredin, R. H. Hauge, and J. L. Margrave, J. Chem. Phys. **77**, 1626 (1982).